Crystal Structure of Human Quinone Reductase Type 2, a Metalloflavoprotein[†,‡]

Christine E. Foster,[§] Mario A. Bianchet,[§] Paul Talalay,[||] Qinjian Zhao,[||] and L. Mario Amzel*[,§]

Departments of Biophysics and Biophysical Chemistry and of Pharmacology and Molecular Sciences, The Johns Hopkins University School of Medicine, 725 North Wolfe Street, Baltimore, Maryland 21205

Received April 7, 1999; Revised Manuscript Received June 1, 1999

ABSTRACT: In mammals, two separate but homologous cytosolic quinone reductases have been identified: NAD(P)H:quinone oxidoreductase type 1 (QR1) (EC 1.6.99.2) and quinone reductase type 2 (QR2). Although QR1 and QR2 are nearly 50% identical in protein sequence, they display markedly different catalytic properties and substrate specificities. We report here two crystal structures of QR2: in its native form and bound to menadione (vitamin K_3), a physiological substrate. Phases were obtained by molecular replacement, using our previously determined rat QR1 structure as the search model. QR2 shares the overall fold of the major catalytic domain of QR1, but lacks the smaller C-terminal domain. The FAD binding sites of QR1 and QR2 are very similar, but their hydride donor binding sites are considerably different. Unexpectedly, we found that QR2 contains a specific metal binding site, which is not present in QR1. Two histidine nitrogens, one cysteine thiol, and a main chain carbonyl group are involved in metal coordination. The metal binding site is solvent-accessible, and is separated from the FAD cofactor by a distance of about 13 Å.

Quinone reductase type 2 (QR2)[1] is expressed in various mammalian tissues, including heart, liver, skeletal muscle, and kidney (1). It was first purified and characterized as a flavoprotein quinone reductase in 1961 (2, 3). Recently, interest in QR2 has resurged with the discovery of its homology to NAD(P)H:quinone reductase type 1 (QR1) (4), an enzyme involved in the catabolism of xenobiotics. Both quinone reductases are cytosolic enzymes, and are active as homodimers, containing one FAD cofactor bound per subunit. QR2 is smaller than QR1, lacking 47 C-terminal amino acid residues. The protein sequences of human QR1 and QR2 can be aligned without insertions or deletions, and are 49% identical over their shared length.

QR1 has long aroused interest in the pharmacological community for its role in protecting mammalian cells against quinone toxicity (5−7). For example, it was recently established that QR1-null mice are more susceptible to quinone toxicity (8). In contrast with other cellular reductases, QR1 catalyzes strict two-electron reductions (9), thereby diverting quinones from one-electron reductions that lead to redox cycling (with concomitant production of deleterious oxygen species) and/or depletion of intracellular glutathione. Induction of QR1 and other phase 2 detoxification enzymes has been demonstrated in response to various chemicals, including isothiocyanates, which are present in broccoli and other cruciferous vegetables (10). QR1 is also involved in the reductive bioactivation of certain chemotherapeutic quinones, including mitomycin-C (11). As many tumors have high, constitutive expression of QR1, the enzyme has become a target for the development of novel chemotherapeutic agents.

Although QR2 is expressed in many of the same tissues as QR1 (1), it does not appear to be induced in conjunction with QR1 (4). In addition, while QR1 reduces quinones using reducing equivalents from NADH or NADPH, QR2 is unable to use such conventional phosphorylated nicotinamides as reductants, and has been shown to react only with a specific subset of nonphosphorylated nicotinamide derivatives, including *N*-methyl, *N*-ribosyl-, and *N*-phenyldihydronicotinamide (2−4). Furthermore, QR2 is only marginally inhibited by characteristic QR1 inhibitors, but is potently inhibited by polycyclic aromatic hydrocarbons (4, 12). These and other factors have made it difficult to identify the physiological function of QR2.

To explore the unique specificity of QR2 as a way of gaining insight into its physiological function, we have determined the high-resolution structure of the human enzyme by X-ray diffraction. Crystals of the native enzyme diffracted to 2.1 Å, and those complexed with menadione (vitamin K_3) diffracted to greater than 2.5 Å. Menadione is a true substrate, and is reduced in vitro by QR2 in the presence of *N*-methyldihydronicotinamide (4). Initial phases for the QR2 model were obtained by molecular replacement, using the previously determined structure of rat QR1 (13). The overall fold of QR2 was found to be very similar to

[†] Supported by National Institutes of Health Grant R01GM45540A to L.M.A. C.E.F. was also supported by National Institutes of Health Training Grant 5T32 GM07445. P.T. was supported by Grant PO1 CA 44530 from the National Cancer Institute, Department of Health and Human Services, and by The Burroughs Wellcome Fund (Morrisville, NC). Q.Z. was supported by National Cancer Institute Fellowship 5T32 CA009243.

[‡] Crystallographic coordinates have been deposited in the RCSB Protein Data Bank with the accession codes 1qr2 and 2qr2.

* To whom correspondence should be addressed. Phone: (410) 955-3955. Fax: (410) 955-0637. E-mail: mario@neruda.med.jhmi.edu.

[§] Department of Biophysics and Biophysical Chemistry.

[||] Department of Pharmacology and Molecular Sciences.

[1] Abbreviations: QR1, NAD(P)H:quinone oxidoreductase type 1 (formerly known as DT-diaphorase); QR2, quinone reductase type 2; FAD, flavin adenine dinucleotide; NAD(P)H, NADH and/or NADPH; ICP-MS, inductively coupled plasma mass spectrometry.

10.1021/bi990799v CCC: $18.00
Published on Web 07/16/1999

Table 1: Crystallographic Data Statistics

	native	menadione
total observations	171959	101551
unique reflections	27290	18052
overall completeness (last shell), %	90.9 (75.7)	97.6 (85.8)
overall R_{sym}[a] (last shell), %	5.70 (24.4)	8.50 (46.5)
unit cell dimensions	$a = 83.2$ Å, $b = 106$ Å, $c = 56.6$ Å, $\alpha = \beta = \gamma = 90°$	$a = 83.6$ Å, $b = 106$ Å, $c = 56.1$ Å, $\alpha = \beta = \gamma = 90°$

[a] $R_{sym} = \sum_{hkl}|(I(hkl)) - I(hkl)|/\sum_{hkl}(I(hkl))$.

that of QR1, although QR2 lacks the small C-terminal domain of QR1. The FAD binding site was also very conserved. In contrast, there were marked differences in residues comprising the NAD(P)H binding site, particularly among those involved in binding the adenosine diphosphate moiety. Surprisingly, QR2 was found to contain a metal binding site which is not present in QR1.

EXPERIMENTAL PROCEDURES

Crystallization and Data Collection. QR2 was purified from *Escherichia coli* expressing human QR2 as described (4). Cell extracts were fractionated by ion-exchange chromatography on a Q-Sepharose Fast Flow column. Further purification was achieved by hydrophobic chromatography using a Phenyl-Superose Fast Flow column. Protein solution (approximately 15 mg/mL) was mixed with an equal volume of reservoir solution (1.4 M ammonium sulfate in 100 mM Na-HEPES, pH 7.0, 12 μM FAD, 1 mM dithiothreitol) and equilibrated over the reservoir. Additionally, protein was cocrystallized with 200 μM menadione using a similar reservoir solution (1.66 M ammonium sulfate in 10 mM Na-HEPES, pH 7.0, 12 μM FAD, 5 mM dithiothreitol). Crystals were formed at 18 °C by vapor diffusion using the hanging-drop technique. X-ray diffraction data were collected at −180 °C with either a Raxis II or a Raxis IV detector using CuKα radiation from a Rigaku RU-200 rotating anode. Reflections were processed using the programs DENZO and SCALEPACK (14). Relevant details are listed in Table 1.

Structure Determination and Refinement. The structure was determined by molecular replacement with the program AMORE (15), using the first 232 residues (all atoms) of rat QR1 (1qrd of the Protein Data Bank) (13) as the search model. Reflections from 15 to 3 Å were used in the search. Independent searches using either the template monomer or the dimer yielded the same solution. The latter result, with an *R*-value of 47.3%, was used as the starting QR2 structure.

A randomly selected portion (10%) of the data was set aside and used for calculating the free *R*-value (16). Visualization of electron density maps and model building were done on an SGI work station using the program O (17). The initial QR2 model was generated by replacing the QR1 sequence with the residues present in QR2. Positional and *B*-factor refinement was done with X-PLOR (18). Water molecules were added when the *R*-value dropped below 25%. Noncrystallographic symmetry restraints were employed throughout the refinement. The metal site geometry was not restrained. The atomic scattering factors employed in modeling the metal site were those of Zn^{2+}. Stereochemical quality was monitored with the program PROCHECK (19). All figures were created using Molscript (20), BobScript (21), and Raster3D (22).

RESULTS

Structure Solution and Refinement. Both native and menadione-bound enzyme crystallized in space group $P2_12_12_1$. The cell dimensions of the two crystals used in data collection were identical within experimental error (Table 1). Native crystals diffracted to 2.1 Å, while those cocrystallized with menadione diffracted to better than 2.5 Å. Representative portions of the electron density maps are shown in Figure 1. The asymmetric units contain one physiological dimer, with the two polypeptide chains related by 2-fold noncrystallographic symmetry. The rms deviation between the two monomers was 0.34 Å for α-carbon atoms in the native structure.

For both structures reported, the *R*-value was 22% or better, and reasonable stereochemistry was observed (Table 2). A Ramachandran diagram placed 88.4% and 89.0% of all residues in the most favored regions for native and menadione-bound structures, respectively.

Description of the Structure and Comparison with QR1. As expected, the overall topology of QR2 is similar to that of QR1 (Figure 2A). Each QR1 monomer can be divided into two domains: a major catalytic domain (residues 1−220) and a much smaller C-terminal domain (residues 221−277). QR2, with 230 residues, contains the N-terminal catalytic domain (5 central, parallel β-strands, flanked on each side by helices), but entirely lacks the C-terminal domain of QR1 (Figure 2B). The 10 C-terminal residues of QR2 (residues 221−230) have no sequence homology with corresponding residues in QR1. In the crystal structure, these 10 residues form a well-defined loop which is divergent in structure from the corresponding residues in QR1 (Figure 3B). Contained within this QR2 C-terminal loop is the cysteine residue which participates in metal coordination (see below).

Coordination of Metal Ion. A metal binding site not present in QR1 was discovered during refinement of the QR2 structure. A strong peak (greater than 7σ) was visible in $F_o - F_c$ difference maps in the vicinity of Cys^{222} in both monomers (Figure 3A). This density was interpreted as indicating the presence of a metal in the QR2 structure. The metal site is tetracoordinate, with two histidine (Nδ) ligands and one cysteine (Sγ) ligand; the fourth ligand is the main-chain carbonyl oxygen of the same cysteine residue. The site exhibits distorted tetrahedral geometry (Table 3). The two histidine ligands, His^{173} and His^{177}, are in adjacent turns of the same α-helix, with their side chains exposed on the same face of the helix; the cysteine ligand is within the unique C-terminal loop (Figure 3B). These ligands comprise

[2] Published amino acid sequences of human (1) and porcine (23) QR2 include the three-residue motif implicated in metal binding. Additionally, mouse QR2 sequences deposited in dbEST (24) possess this motif, and partial rat QR2 EST's have His^{177} and Cys^{222}.

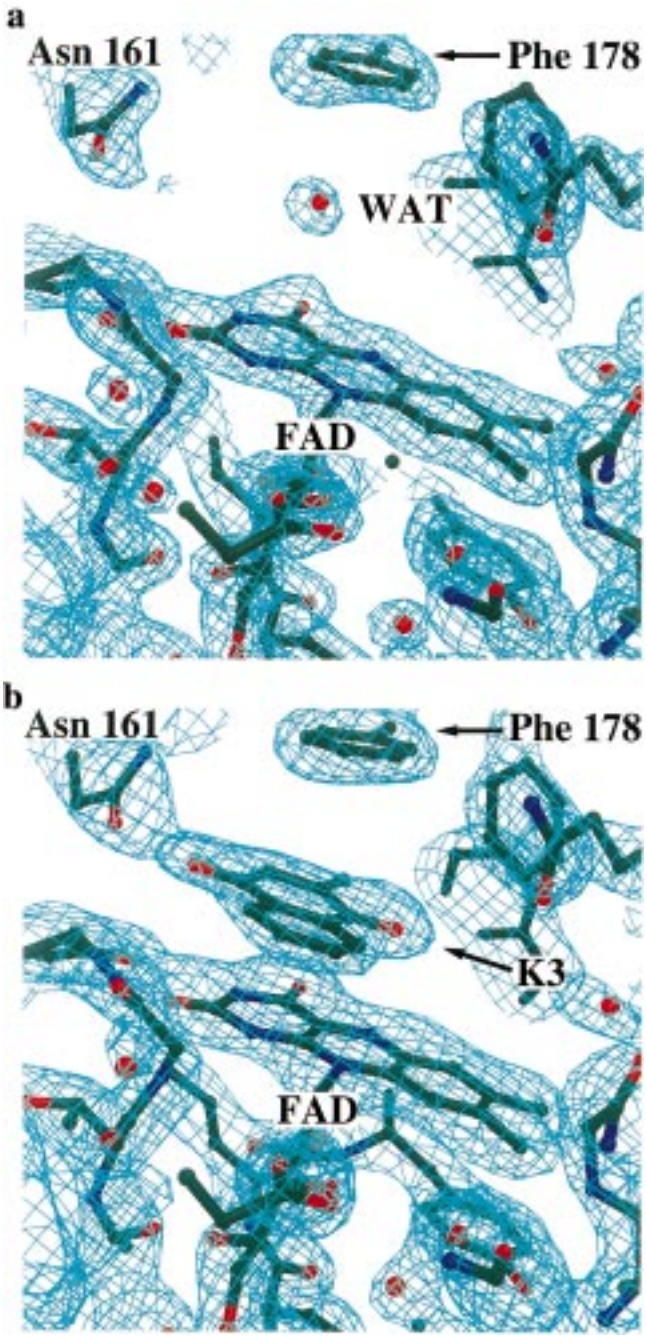

FIGURE 1: Final $2F_o - F_c$ maps of the active site contoured at 1.2s. (A) Native QR2 at 2.1 Å. (B) Menadione bound to QR2 at 2.5 Å.

a three-residue motif which is present in all QR2 sequences known,[2] but not in QR1 sequences.

Cofactor Binding Site. QR2 contains two molecules of FAD, which are bound at opposite ends of the dimer interface. The conformations and locations of QR1- and QR2-bound FAD are very similar, with an rms deviation of 0.91 Å. In both enzymes, tight binding of FAD is achieved through multiple protein contacts. Almost all of these specific contacts are identical in QR1 and QR2. The isoalloxazine moiety is anchored by hydrogen bonds to main-chain NH groups of $Trp^{105,}$ Phe^{106}, Gly^{149}, and Gly^{150}, and to the side chain of Tyr^{155}. Also, the carbonyl oxygen of Leu^{103} contacts N5 of the isoalloxazine ring. The side chain of Tyr^{104} is stacked with the dimethyl ring of the flavin. Oxygen atoms O2* and O4* in the ribitol portion of FAD interact with the main-chain carbonyl oxygen of Leu^{103} and the side chain of Thr^{147}, respectively. In QR2, there is an additional contact, not observed in QR1, between O3* and the side chain of Glu^{193}. Protein interactions with the first phosphate group are also preserved in QR2: O2P is hydrogen-bonded to both the backbone and side-chain nitrogens of Asn^{18}, and O1P contacts both the side chain of His^{11} and a water molecule. In QR1, there is a hydrogen bond between Gln^{66} and the second phosphate group of FAD, but in QR2 this contact is lost due to the substitution of glutamine by asparagine. As in QR1, the adenine ring is contacted by the side chains of Arg^{200} and Glu^{197}, and by the main-chain NH group of Phe^{17}. In summary, of the 13 residues employed by QR1 for FAD binding, only 1 (Gln^{66}) is mutated in QR2.

Table 2: Quality of the Final Model

	native	menadione
refinement maximum resolution, Å	2.10	2.45
R-value (free *R*-value), %	21.9 (28.4)	21.2 (27.3)
no. of non-hydrogen protein atoms	4034	4034
no. of FAD atoms	128	128
no. of menadione atoms	N/A	26
no. of waters	195	90
average *B*, Å^2		
protein atoms	23.7	32.6
FAD atoms	37.8	28.0
menadione atoms	N/A	37.1
waters	30.2	34.6
metal ions	26.5	54.6
rms deviations from ideal geometry		
bond lengths, Å	0.016	0.018
bond angles, deg	2.07	1.29
improper dihedral angles, deg	1.67	1.15
Protein Data Bank entry code	1qr2	2qr2

Menadione Binding Site. In the model obtained from QR2 cocrystallized with menadione, similar patches of electron density were observed in the active sites of both monomers, parallel to the plane of the isoalloxazine ring. Although menadione was successfully modeled into this density, the orientation of the molecule was somewhat ambiguous. We have placed it so that the substituted ring of menadione is stacked with ring A of the FAD, with one of the menadione oxygens located 3.3 Å from N5 of the FAD (Figure 1B). The nonsubstituted ring of menadione stacks with ring B of the FAD. Menadione binding does not seem to be associated with significant conformational changes in the protein, as the structures of native and menadione-bound QR2 are very similar (rms deviation of 0.17 Å for α-carbons).

DISCUSSION

QR2 has been termed the "long-forgotten flavoenzyme" (4), having been recently rediscovered with the identification of its genetic relationship to the well-studied QR1. Although QR1 and QR2 each catalyze two-electron reductions of quinones, the precise degree of functional overlap is not clear. QR2 exhibits distinct kinetic and inhibition properties and cannot react with QR1 electron donors, such as NADH and NADPH. Instead it was found to react with nonphosphorylated nicotinamides. The structures of QR2 presented here provide important clues about its function and mechanism. Most importantly, the conservation of catalytic site residues, detailed below, suggests that both enzymes utilize similar catalytic mechanisms. One important characteristic shared by both enzymes is the utilization of the same binding site

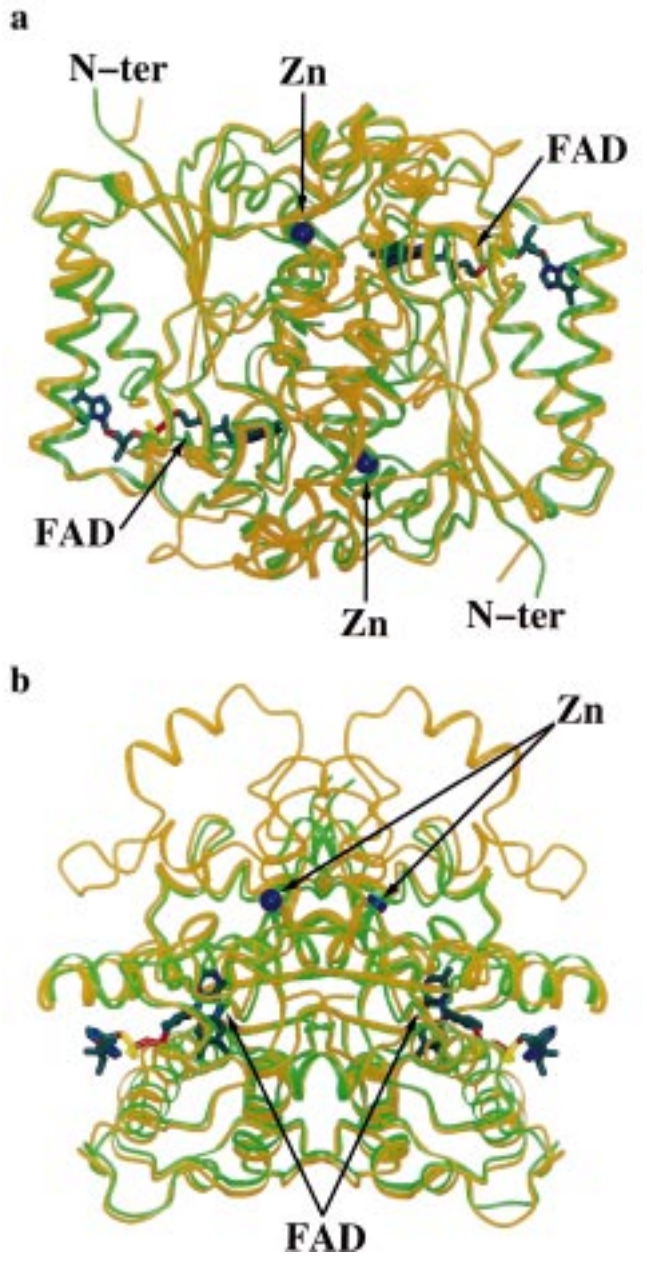

FIGURE 2: Superposition of QR1 and QR2. Two views of the aligned structures of rat QR1 (orange) and human QR2 (green) are shown. (A) The common catalytic domain, present in both QR1 and QR2, is evident. (B) The small C-terminal domain (present only in QR1) is evident (top of panel). QR2-bound zinc ions are in blue. Only the FAD molecules bound by QR2 are shown for clarity.

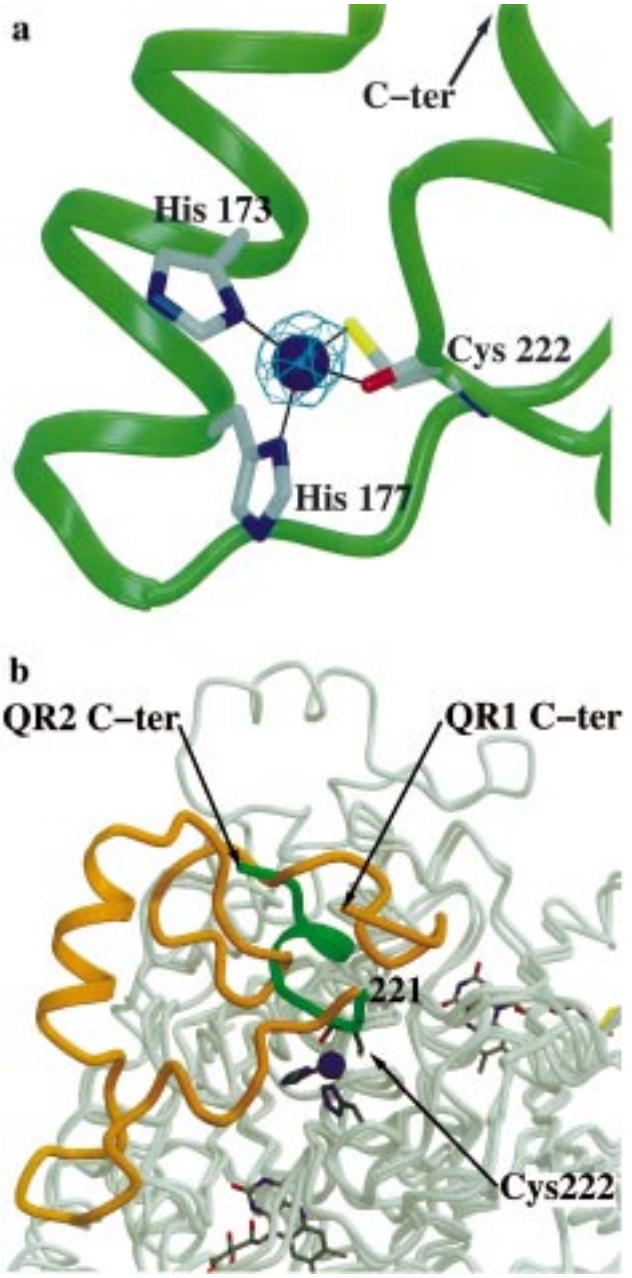

FIGURE 3: Metal binding site. (A) Zinc atom (blue) and interactions with protein ligands (solid lines). A final omit map ($F_o - F_c$), with the zinc atom omitted, is shown in aqua. The map is contoured at 6.0σ. (B) Comparison of QR1 and QR2 structures in the vicinity of the metal site. The C-termini (from residue 221) are colored; the shared catalytic domains are in gray. The C-terminus of QR2 (green) is a 10-residue loop which contains Cys^{222}, 1 of the metal ligands; the C-terminus of QR1 (orange) is 53 residues long.

for substrate and for the source of reducing equivalents. In QR1, this results in ping-pong kinetics (25), and similar kinetics are expected for QR2 using alkyl-nicotinamides as reductants. Several of these aspects are discussed below.

Role of Metal in QR2. Metal ions in proteins have been implicated in nucleophilic catalysis (carboxypeptidase, carbonic anhydrase, alcohol dehydrogenase), structural stabilization (alcohol dehydrogenase, zinc finger proteins), and electron transfer (rubredoxin, azurins, cytochromes). The first challenge in assigning a role for QR2-bound metal is to determine the endogenous metal. ICP-MS analyses on FPLC-purified enzyme have identified the metal ion bound in our QR2 preparation as zinc (Holtzclaw, W. D., Zhao, Q., Foster, C. E., and Talalay, P., Johns Hopkins University School of Medicine, unpublished results). However, it is not clear whether zinc is the in vivo metal, or results from expressing the protein in a bacterial system. Incorporation of non-native metals after heterologous expression has been previously observed; for example, expression of *Pseudomonas aeruginosa* copper azurin in *Escherichia coli* also produces zinc azurin (26). In the case of human superoxide dismutase, the metal ion chaperone protein Ccs is required for incorporation of copper (27).

The coordination system of the QR2 metal site can be compared with the metal sites of other enzymes. The coordination seen in QR2 is most similar to type I Cu sites, which almost exclusively serve electron-transfer functions in enzymes. Type I Cu sites, best exampled by the blue

Table 3: Geometry of the Metal Site[a]

bonds	Å
Zn−His^{173} (Nδ)	2.22 ± 0.047
Zn−His^{177} (Nδ)	2.02 ± 0.052
Zn−Cys^{222} (Sγ)	2.21 ± 0.042
Zn−Cys^{222} (O)	2.25 ± 0.025
angles	**deg**
His^{177} (Nδ)−Zn−His^{173} (Nδ)	115 ± 0.37
His^{177} (Nδ)−Zn−Cys^{222} (Sγ)	116 ± 4.4
Cys^{222} (Sγ)−Zn−His^{173} (Nδ)	121 ± 3.4
Cys^{222} (O)−Zn−Cys^{222} (Sγ)	98.4 ± 1.3
Cys^{222} (O)−Zn−His^{173} (Nδ)	102 ± 0.76
Cys^{222} (O)−Zn−His^{177} (Nδ)	96.4 ± 1.4

[a] Values reported are the average of both monomers in the native (2.1 Å) model.

copper proteins, involve two His (Nδ), one Cys (Sγ), and a fourth variable ligand (Met in the case of plastocyanins and azurins). In QR2, the metal is also coordinated by two His Nδ atoms and one Cys residue. However, the QR2 metal site is uncharacteristic of type I copper sites in that Cys^{222} contributes *two* ligands: the Sγ and the carbonyl O. Furthermore, His^{173} and His^{177} are unusually close in the primary sequence (personal communication, S. Karlin, Department of Mathematics, Stanford University).

Although the greatest similarity exists between the metal site of QR2 and type I Cu sites, there are also similarities with Zn sites. Zinc also forms tetracoordinate complexes, involving nitrogen, oxygen, and sulfur atoms, and specifically those in His, Asp/Glu, and Cys residues. The most similar to QR2 are class IV Zn sites, which also involve two His; however, one coordination position is always occupied by water (28).

For several reasons we consider it likely that QR2 is a copper enzyme, and that the metal site may be linked to the active site by an electron-transfer route. The QR2 metal site is similar to that seen in copper enzymes functioning in electron transfer. Furthermore, the location of the metal on the protein surface renders unlikely a role in structural stabilization, but is consistent with a role in electron transfer.

Pathway Analysis of QR2 Structure. Potential pathways for electron transfer between the FAD and metal sites of QR2 were analyzed using the Greenpath v0.97 computer program (29). A representative pathway is illustrated in Figure 4. Predicted pathways involved a combination of through-bond and through-space interactions, and similar results were observed for both FAD/metal pairs in the dimer.

Catalytic Site. (i) General Description of the Catalytic Site. In the QR2 dimer, there are two equivalent catalytic sites, located far from each other at opposite ends of the dimer interface. Each site is a large cavity, lined by residues from both monomers. The isoalloxazine rings are bound deep inside the cavities and form the floor of the catalytic sites. Several differences can be noted in the catalytic sites of QR1 and QR2. In QR1, Tyr^{126} and Tyr^{128} are positioned within the active site with their side chains perpendicular to the plane of the FAD isoalloxazine ring. These two tyrosines are replaced in QR2 by Phe^{126} and Ile^{128}. Furthermore, Met^{131} is replaced by Phe^{131} in QR2. As a result, the active site cavity of QR2 is slightly larger and more hydrophobic than that of QR1. These changes must be responsible for the observed differences in substrate and inhibitor specificity between the two enzymes.

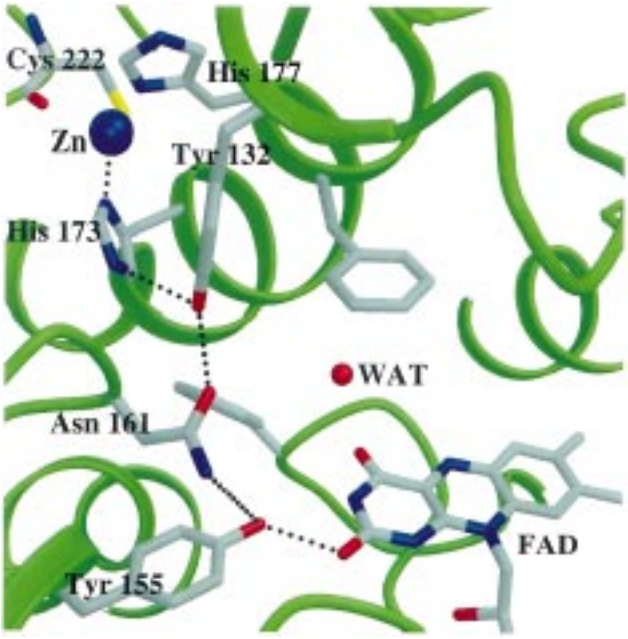

FIGURE 4: Possible pathway for intramolecular electron transfer. Shown is one potential route between FAD and metal bound by QR2. The pathway (dashed lines) involves a combination of through-bond and through-space interactions, including those between hydrogen-bonded residues.

(ii) Binding of Electron Donors. In QR1, binding sites for electron donor and quinone acceptor are nearly overlapping. Binding of NAD(P)H by QR1 occurs in one of two orientations, one of which involves multiple hydrogen bonds between cofactor and protein (13). In both orientations, additional stabilization is provided by aromatic stacking of the nicotinamide ring with ring C of the FAD isoalloxazine moiety. In contrast to the high conservation of residues involved in FAD binding, residues involved in NAD(P)H binding in QR1 are not well conserved in QR2. Additionally, protein−cofactor contacts are lost by truncation of the C-terminus. Although aromatic ring stacking can still occur, the loss of specific contacts with the ADP moiety of NAD(P)H likely accounts for the inability of QR2 to react with the phosphorylated hydride donors NAD(P)H.

Nonphosphorylated hydride donors most likely bind QR2 principally through aromatic stacking interactions, as both polar (*N*-ribosyl-) and nonpolar (*N*-phenyl-) N-substituted dihydronicotinamides are tolerated. To date, there is no known mechanism for generating the reduced forms of these nonphosphorylated nicotinamides in vivo, as a mammalian homologue of the bacterial NADH hydrolases has yet to be identified. As a result, the physiological electron donor for QR2 has yet to be definitively assigned.

(iii) Binding of Quinones. The binding of menadione by QR2 is reminiscent of the binding of 2,3,5,6-tetramethylquinone by QR1. There are no specific contacts between protein and substrate, although they are linked by water molecules. Although the orientation of menadione is not entirely certain, it appears that binding in the crystal structure is the productive conformation, with one of the menadione oxygens located near N5 of the FAD.

Mechanism of Quinone Reduction. The obligatory two-electron reduction reaction of QR1 has been proposed to

occur via two direct hydride transfers: one from NAD(P)H to FAD, the other from $FADH_2$ to quinone. Although the possibility of two one-electron transfers has not been definitively ruled out, no experiment has ever indicated the presence of a semiquinone intermediate (9, 25). The mechanism formulated based on the crystal structure (13) involves hydride transfer from C4 of the nicotinamide ring of NAD(P)H to N5 of the flavin ring, followed by a tautomerization leading to placement of the negative charge on the O1P oxygen. Tyr^{155} is hydrogen-bonded to this oxygen, and is thus in position to transfer its OH proton. Tyr^{155} may in turn receive a proton from nearby His^{161}. We have considered whether this mechanism may apply to quinone reduction by QR2. While the active site is largely conserved, including Tyr^{155}, an asparagine replaces His^{161} in QR2. This substitution may be compensated for by a water molecule, although the nearest is 5.2 Å away from the OH group of Tyr^{155} and is hydrogen-bonded to O4 of the flavin. In addition, if the endogenous metal present in QR2 is redox-active, it may be part of a mechanism involving two sequential one-electron transfers from a cytoplasmic, one-electron donor.

Our discovery of a copper-like metal site in QR2 provides clues toward identifying the unique function served by QR2 in mammalian cells. Identification of the in vivo metal will be critical in determining its role in the catalytic mechanism of QR2. Furthermore, crystallization of the enzyme in complex with electron donors should also prove insightful.

REFERENCES

1. Jaiswal, A. K. (1994) *J. Biol. Chem. 269*, 14502−14508.
2. Liao, S., and Williams-Ashman, H. G. (1961) *Biochem. Biophys. Res. Commun. 4*, 208−213.
3. Liao, S., Dulaney, J. T., and Williams-Ashman, H. G. (1962) *J. Biol. Chem. 237*, 2981−2987.
4. Zhao, Q., Yang, X. L., Holtzclaw, W. D., and Talalay, P. (1997) *Proc. Natl. Acad. Sci. U.S.A. 94*, 1669−1674.
5. Benson, A. M., Hunkeler, M. J., and Talalay, P. (1980) *Proc. Natl. Acad. Sci. U.S.A. 77*, 5216−5220.
6. Talalay, P. (1989) *Adv. Enzyme Regul. 28*, 237−250.
7. Talalay, P., Fahey, J. W., Holtzclaw, W. D., Prestera, T., and Zhang, Y. (1995) *Toxicol. Lett. 82/83*, 173−179.
8. Radjendirane, V., Joseph, P., Lee, Y.-H., Kimura, S., Klein-Szanto, A. J. P., Gonzalez, F. J., and Jaiswal, A. K. (1998) *J. Biol. Chem. 273*, 7382−7389.
9. Iyanagi, T., and Yamazaki, I. (1970) *Biochim. Biophys. Acta 216*, 282−294.
10. Fahey, J. W., Zhang, Y., and Talalay, P. (1997) *Proc. Natl. Acad. Sci. U.S.A. 94*, 10367−10372.
11. Ross, D., Siegel, D., Beall, H., Prakash, A. S., Mulcahy, R. T., and Gibson, N. W. (1993) *Cancer Metastasis Rev. 12*, 83−101.
12. Liao, S., and Williams-Ashman, H. G. (1961) *Biochem. Pharmacol. 6*, 53−54.
13. Li, R., Bianchet, M. A., Talalay, P., and Amzel, L. M. (1995) *Proc. Natl. Acad. Sci. U.S.A. 92*, 8846−50.
14. Otwinowski, Z., and Minor, W. (1997) *Methods Enzymol. 276*, 307−326.
15. Navaza, J. (1994) *Acta Crystallogr. A 50*, 157−163.
16. Brünger, A. T. (1992) *Nature 355*, 472−475.
17. Jones, T. A., Zou, J. Y., Cowan, S. W., and Kjeldgaard, M. (1991) *Acta Crystallogr. A 47*, 110−119.
18. Brünger, A. T. (1992) *X-PLOR Version 3.1: A System for X-ray Crystallography and NMR*, Yale University Press, New Haven, CT.
19. Laskowski, R. A., MacArthur, M. W., Moss, D. S., and Thornton, J. M. (1993) *J. Appl. Crystallogr. 26*, 283−291.
20. Kraulis, P. J. (1991) *J. Appl. Crystallogr. 24*, 946−950.
21. Esnouf, R. M. (1997) *J. Mol. Graphics 15*, 132−134.
22. Merritt, E. A., and Bacon, D. J. (1997) *Methods Enzymol. 277*, 505−524.
23. Kodama, T., Wakui, H., Komatsuda, A., Imai, H., Miura, A. B., and Tashima, Y. (1997) *Nephrol. Dial. Transplant. 12*, 1453−1460.
24. Boguski, M. S., Lowe, T. M., and Tolstoshev, C. M. (1993) *Nat. Genet. 4*, 332−333.
25. Tedeschi, G., Chen, S., and Massey, V. (1995) *J. Biol. Chem. 270*, 1198−1204.
26. Nar, H., Huber, R., Messerschmidt, A., Filippou, A. C., Barth, M., Jaquinod, M., van de Kamp, M., and Canters, G. W. (1992) *Eur. J. Biochem. 205*, 1123−1129.
27. Culotta, V. C., Klomp, L. W. J., Strain, J., Casareno, R. L. B., Krems, B., and Gitlin, J. D. (1997) *J. Biol. Chem. 272*, 23469−23472.
28. Karlin, S., Zhu, Z. Y., and Karlin, K. D. (1997) *Proc. Natl. Acad. Sci. U.S.A. 94*, 14225−14230.
29. Regan, J. J., Risser, S. M., Beratan, D. N., and Onuchic, J. N. (1993) *J. Chem. Phys. 97*, 13083−13088.

BI990799V